Transactions of the Korean Nuclear Society Spring Meeting
Jeju, Korea, May 18-19, 2017

Creep Crack Growth Behavior of Candidate Materials for Use in a VHTR System

Woo-Gon Kim[a*], Jae-Young Park[a], Eung-Seon Kim[a], Yong-Wan Kim[a], Min-Hwan Kim[a]
[a] *Korea Atomic Energy Research Institute, 989-111, Daedeokdaero, Yuseong, Daejeon, Korea, 305-353*
[*]*Corresponding author: wgkim@kaeri.re.kr*

1. Introduction

A very high temperature reactor (VHTR) is one of the most promising Gen-IV reactors for the economic production of electricity and hydrogen. Its major components are the reactor internals, reactor pressure vessel (RPV), hot gas ducts (HGD), and intermediate heat exchangers (IHX). Alloy 617 is a prime candidate material for the IHX component, and Grade 91 steel (hereafter Gr. 91) is also a candidate material for the RPV component [1, 2]. Since the VHTR components are designed to be used for a 60 year lifetime at a high temperature, their components are subjected to a non-uniform stress and temperature distribution during service. These conditions generate localized creep damage and propagate the cracks and ultimately cause a fracture. A significant portion of the components' life can be spent in crack propagation. Thus, it is very important to evaluate the creep crack growth rate (CCGR) from a design concern and in predicting the residual life of the components during the high temperature service [3, 4].

Efforts are now being undertaken in the Generation IV program to provide data needed for the design and licensing of the nuclear plants, and with this goal in mind, to meet the needs of the conceptual designers of the VHTR system, "Gen-IV Materials Handbook database(DB)" is being established through an international collaboration program of several GIF (Gen-IV Forum) countries. However, the creep crack growth rate (CCGR) data for Alloy 617 and Gr. 91 steel are not available in the ASME code. Therefore, the experimental data for CCG behavior should be prepared to establish "the Gen-IV Materials Handbook DB" for design use of the components.

In this paper, the CCG behavior for Alloy 617 and Gr. 91 steel was investigated using the CCG data obtained for different applied loads at 800 and 850^{o}C for Alloy 617 and at 600^{o}C for Gr. 91 steel. For Gr. 91 steel, the CCGR laws were compared with base metal (BM), weld metal (WM), and heat affected zone (HAZ) at 600^{o}C. The CCGR was calculated in terms of C^* fracture parameter. In addition, a probabilistic analysis for evaluating CCGR was introduced using Monte-Carlo simulation.

2. Methods and Results

2.1 Experimental procedures

To obtain the material constants being used in the C^* equation, tensile and creep tests were performed at each temperature. Tensile test specimens were machined with a rectangular cross section of 28.5 mm in gage length, 6.25 mm in width, and 1.5 mm in thickness. The strain rate in the tensile tests was conducted with a slow strain rate of 5.85E-4 (1/s) at each temperature. Also, creep test specimens were machined with a cylindrical form of 30 mm in gauge length and 6 mm in diameter. A series of creep tests was performed under different stress levels at each temperature. The pull rod and jig used in the creep tests were manufactured with Ni-base superalloy materials to endure oxidation and thermal degradation sufficiently during the creep tests at the high temperature above 800^{o}C. Creep strain data with elapsed times were taken automatically by a PC through a high precision LVDT.

Creep crack growth tests were performed with different applied load levels at each temperature. The compact tension (CT) specimens had a width (W) of 25.4mm, thickness (B) of 12.7mm, and side grooves with a 10% depth. The initial crack ratio (a/W) was about 0.5. The pre-cracking size was 2.0mm and was machined by an EDM to introduce a sharp crack tip starter. Load-line displacement (LLD) data were measured using a linear gauge assembly attached to the specimen, and the crack length was determined using a direct current potential drop (DCPD) method. The crack length was calculated using the Johnson's formula from the results of the DCPD. After the CCG testing, the CT specimens were cooled down in a liquid nitrogen solution and fractured to measure the final crack length.

2.2 Determination of tensile and creep constants

The *D* and *m* constants were obtained from the tensile tests at 800 and 850^{o}C for Alloy 617 and at 600^{o}C for Gr. 91 steel. Tensile plastic constants were obtained by Ramberg-Osgood (R-O) equation of $\varepsilon_p = D(\sigma/\sigma_{ys})^m$. The *A* and *n* values were determined from creep tests at each temperature for Alloy 617 and Gr. 91 steel. Also, the creep constants for two materials at each temperature were obtained by Norton's power law of $\dot{\varepsilon}_{ss} = A\sigma^n$. The *D*, *m*, *A*, and *n* constants at each temperature for two materials were obtained, respectively. The values obtained for four constants at each temperature were used in calculation of the C^* parameter. Typical results obtained for the tensile and creep constants of Alloy 617 are presented in Figs. 1 and 2.

Fig. 1 is a typical result of log (plastic strain) vs. log (σ/σ_{ys}) to determine the *D* and *m* values for Alloy 617 at 800^{o}C. Fig. 2 is a typical result of log (creep rate) vs. log (stress) to determine the *A* and *n* values for Alloy

617 at 800 and 850°C. The creep rate of 850°C is faster than that of 800°C. The creep exponent is similar as n=6.5 at two temperatures.

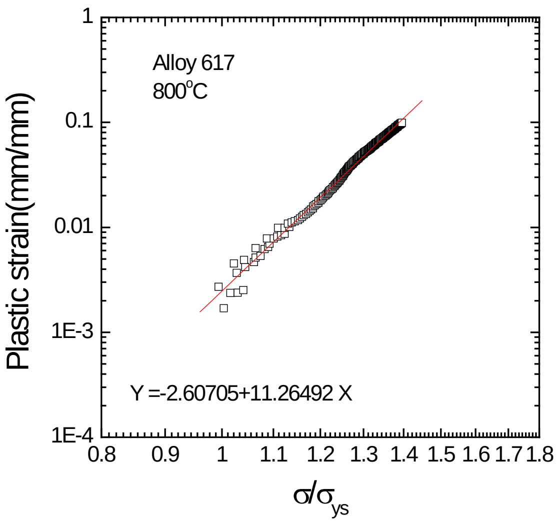

Fig. 1. A typical result showing log (plastic strain) vs. log (σ/σ_{ys}) to determine D and m values for Alloy 617 at 800°C.

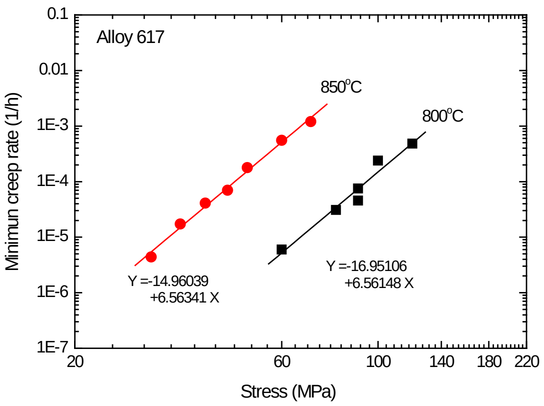

Fig. 2. A typical result showing log (creep rate) vs. log (stress) to determine the A and n values for Alloy 617 at 800 and 850°C.

2.3 CCGR laws

Fracture mechanics parameter, C^*-integral has been widely used to characterize the CCGR in metals undergoing a steady state creep. The general form between the CCGR (da/dt) and the C^* can be expressed as the following Eq. (1) [4-6],

$$da/dt = B[C^*]^q \tag{1}$$

where n is the creep exponent, and B and q coefficients are material constants. They are related to the intercept and slope, respectively. For the CT specimen, the C^* value was calculated by Eq. (2), and load-line displacement rate ($\dot{V}_c$) due to creep strain was calculated by Eq. (3) [7].

$$C^* = \frac{P\dot{V}_c}{B_N(W-a)}\eta\left(\frac{a}{W}, n\right) \tag{2}$$

$$\dot{V}_c = \dot{V} - \frac{\dot{a}B_N}{P}\left(\frac{2K^2}{E} + (m+1)J_p\right) \tag{3}$$

where P = applied load, a = crack size, W = width of specimen, $\dot{V}$ = total load-line displacement rate, B_N = net thickness of specimen, E= elastic modulus for plane strain, K = stress intensity factor, $\dot{a}$ = crack growth rate, and m = stress exponent. The calculating procedures of the C^* values were conducted according to the ASTM E1457 procedures [7].

Fig. 3 shows a typical result of da/dt vs. C^* parameter obtained for Alloy 617 at 800°C. A CCGR law can be proposed by following equation:

$$da/dt = 1.28\text{x}10^{-2}\cdot(C^*)^{0.91} \tag{4}$$

Consequently, for a given value of C^*, the rate of creep crack propagation can be estimated for Alloy 617 at 800°C. Also, the CCGR law at 850oC was obtained using the identical manner at 800°C, and the CCGR laws was compared at two temperatures. The CCGR at 850°C was investigated to be faster than that of 800°C.

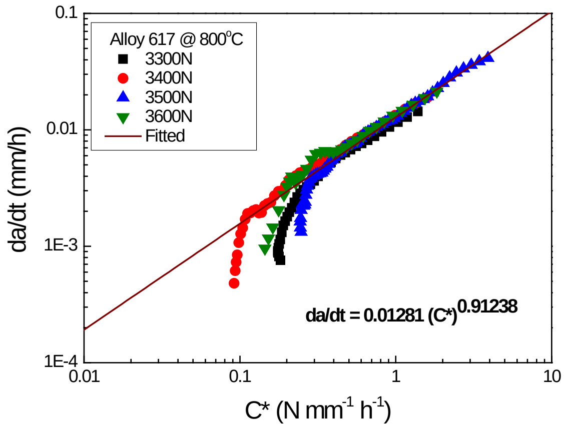

Fig. 3. A typical CCGR line obtained for Alloy 617 at 800°C.

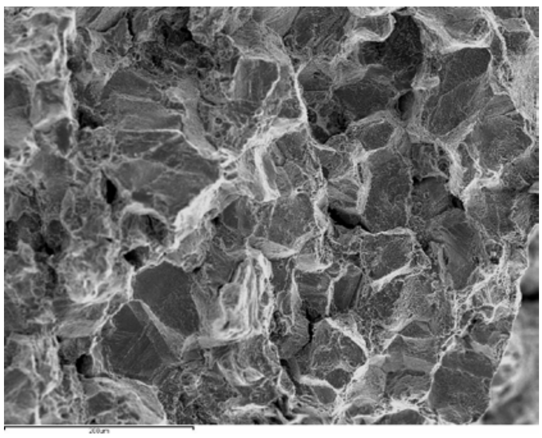

Fig. 4. SEM fracture surface showing typical intergranular fracture mode as observed after the CCG tests under 3400N of Alloy 617 at 800°C.

Fig. 4 shows a typical SEM fracture surface of Alloy 617 fractured after CCG tests under 3400N at 800°C. A dominant fracture mode reveals a typical intergranular fracture, which was generally observed well in creep deformation of Alloy 617. Creep crack growth due to creep damage is found to be developed along the grain boundary as the evidence.

In addition, for Gr. 91 steel, the CCG behaviors were comparatively investigated for BM, WM, and HAZ at 600°C, and their CCGR laws were obtained using the C^* fracture parameter as described above. Fig. 5 shows a comparison of the CCGR lines for the BM, WM, and HAZ of Gr. 91 steel at 600°C. As seen well in Fig. 5, each CCGR law can be proposed by following equations:

$$\text{BM: } da/dt = 1.89\text{x}10^{-2}\cdot(C^*)^{0.77}, \quad (5)$$

$$\text{WM: } da/dt = 3.62\text{x}10^{-2}\cdot(C^*)^{0.85}, \quad (6)$$

$$\text{HAZ: } da/dt = 3.70\text{x}10^{-2}\cdot(C^*)^{0.86}. \quad (7)$$

As given above, it is found that in the CCGR laws, the WM and HAZ is similar, but they are faster than BM. When the CCGR law of the BM is compered with the data of French SFR design code of RCCMRx, the experimental data was a little faster than RCC-MRx code data. Thus, it is suggested that RCC-MRx code is estimated to be conservertative.

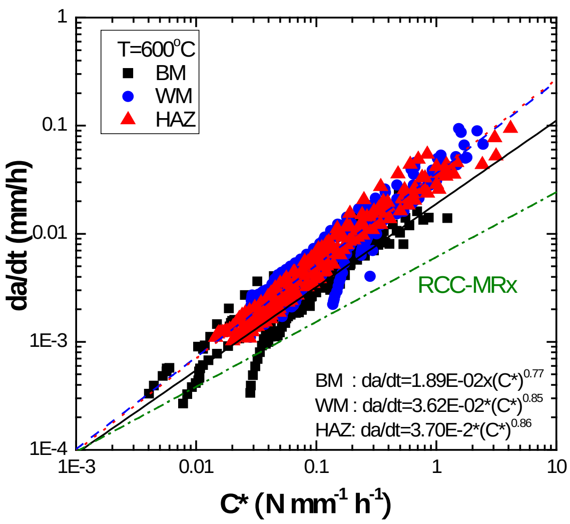

Fig. 5. A comparison of the CCGR lines for the BM, WM, and HAZ of Gr. 91 steel at 600°C.

Fig. 6 shows macro fracture micrograph for crack propagation in front of crack tip in the HAZ region of Gr. 91 steel tested at 600°C. As seen well in the photo, the crack is developed along the HAZ region between BM and WM. This is called as "Type-IV crack" in weldments. Generally, because the F/M steel is known to be the weakest in the HAZ region, the CCGR in the HAZ is reasonable to be faster than that of the BM. In a far distance from crack tip, minor voids are formed owing to creep damage. The cracks will be propagated by linking of the minor voids.

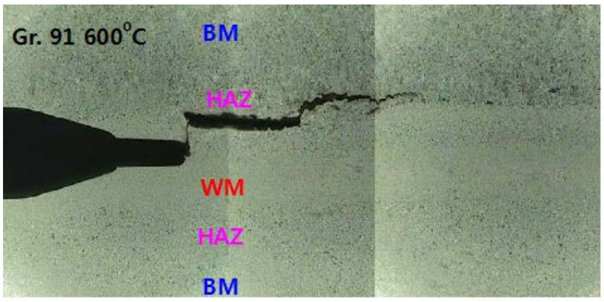

Fig. 6. Optical microscope showing crack propagation in HAZ region of Gr. 91 weldment.

2.4 Probabilistic estimation of the CCGR line

In this study, the CCGR data were dealt with from probabilistic viewpoints to logically evaluate the CCGR. Using the Monte Carlo simulation (MCS) based on probability distribution method (PDM) in the CCGR data, a number of random variables were generated, and the CCGR lines could be predicted probabilistically.

Herein, the MCS was applied to generate the appropriate values of random variables (*i.e.* random numbers) for the B and q coefficients. Box and Muller [8] have proposed that random variables (S) with a standard normal distribution can be represented as,

$$S = (-2\ln U_1)^{0.5}\cos 2\pi U_2 \;. \quad (8)$$

Where, the U_1 and U_2 are standard uniform variables, which have a uniform probability density function (PDF) between 0 and 1.0. Thus, random variables (x) with a normal distribution $N(\mu, SD)$ can be given as [9],

$$x = \mu + SD\cdot S = \mu + SD(-2\ln U_1)^{0.5}\cos 2\pi U_2 \,. \quad (9)$$

For a lognormal random variable x', the distribution of x = log (x') is a normal distribution. Thus, if x is a value generated from Eq. (6),

$$x' = 10^x \;. \quad (10)$$

Eq. (10) becomes a random number for the lognormal distribution with a mean μ and standard deviation SD. Eqs. (9) and (10) were used to generate the values of the B and q, which followed a lognormal distribution well.

Standard uniform variables of the U_1 and U_2 were generated using Eq. (9). The numbers of the random variables were generated for B and q. It was supported that the B and q data followed the lognormal distribution because the data plotted a linear relationship. It was identified that the random variables of the B and q were well realized by the MCS.

Fig. 7 shows a typical result of the MCS of da/dt vs. C^* for Gr. 91 BM at 600°C. Probability distributions were generated for the wide ranges of the C^* values from 0.001 to 10 as shown in Fig. 8. From these distributions, the CCGR lines could be predicted probabilistically.

Fig. 9 shows an example of the probability lines predicted for 90% and 10% obtained from the MCS. It means that that the upper prediction line is for 90% fracture probability and the lower prediction line is for 10% fracture probability.

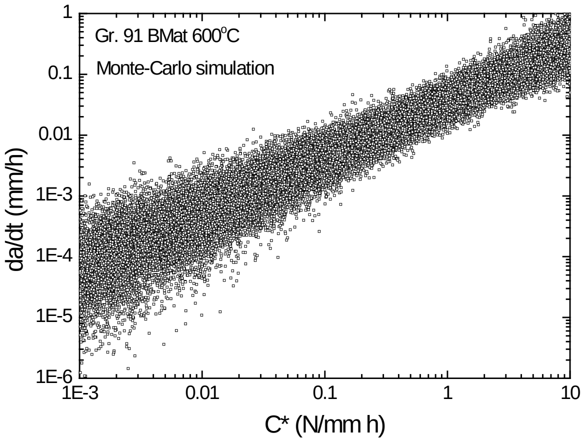

Fig. 7. Large body of CCGR data generated using MCS from lognormal distribution of the *B* and *q*.

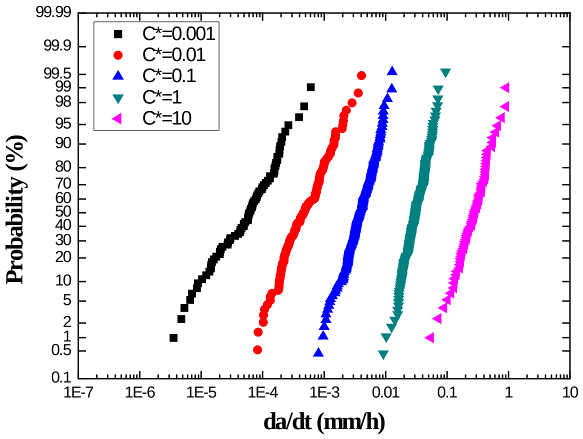

Fig. 8. Probability distributions of the CCGR for various C^* values.

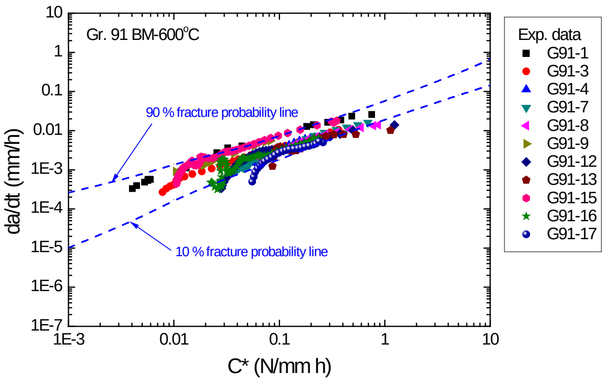

Fig. 9. Probability lines predicted for 90% and 10% obtained from the MCS.

Consequently, using the lognormal distribution investigated for Gr. 91 steel, a number of random variables, *P* (*B*, *q*) with the various C^* values could be realized by the MCS. Then, the CCGR lines were predicted with a probabilistic reliability using the generated random variables.

3. Conclusions

Experimental CCG data of Alloy 617 and Gr. 91 steel were obtained from a series of creep crack growth tests under different applied loads at high temperatures. The CCGR laws for a given value of C^* was constructed for two materials. For the CCGR laws of Gr. 91 weldment, the WM and HAZ were faster than BM, and the CCGR dada of RCC-MRx code were identified to be conservertative. Many data for random variables of *B* and *q* were realized using Monte Carlo simulation, and using the generated data, the CCGR lines could be reasonably predicted for a probabilistic viewpoints.

ACKNOWLEDGEMENTS

This work was supported by the National Research Foundation of Korea (NRF) grant funded by the Korea government (MSIP) (No. 2017M2A8A1014758).

REFERENCES

[1] W.G. Kim, S.N. Yin, G.G. Lee, Y.W. Kim and S.J. Kim, Creep Oxidation Behavior and Creep Strength Prediction for Alloy 617, Int. J. of Pressure Vessels and Piping, Vol. 87, pp. 289-295, 2010.

[2] J.H. Chang, et al., A Study of a Nuclear Hydrogen Production Demonstration Plant, Nuclear Eng. and Tech., Vol. 39, No.2, pp. 111-122, 2007.

[3] W.G. Kim, S.N. Yin, W.S. Ryu, S.J. Kim and W. Yi, Probabilistic Analysis of the Creep Crack Growth Rate of Type 316LN Stainless Steel by the Monte Carlo Simulation, Journal of ASTM International, Vol.3, pp. 71-80, 2006.

[4]K.M. Nikbin, D.J. Smith and G.A. Webster, An Engineering Approach to Prediction of Creep Crack Growth, Transactions of the ASME, Vol. 108, pp.186-191, 1986.

[5]A. Saxena, Nonlinear Fracture Mechanics for Engineers, CRC Press, New York, pp. 363~377, 1997.

[6] T.L. Anderson, Fracture Mechanics, Second Edition, CRC Press, London, pp. 226-228, 1995.

[7]ASTM E1457-00, Standard Test Method for Measurement of Creep Crack Growth Rates in Metals, ASTM Standard, 2000.

[8] G.E.P. Box and M.E. Muller, A Note on the Generation of Random Normal Deviates, Annals of Math. Stat., Vol. 29, pp. 610-611, 1958.

[9]M. Yatomi, Factors Affecting the Failure of Cracked Components at Elevated Temperature, A Thesis for the Ph. D. of Imperial College, pp. 58-59, 2003.